

pubs.acs.org/acschemicalbiology Letters

# A Metabolite Produced by Gut Microbes Represses Phage Infections in *Vibrio cholerae*

Zhiyu Zang, Kyoung Jin Park, and Joseph P. Gerdt\*



Cite This: ACS Chem. Biol. 2022, 17, 2396–2403



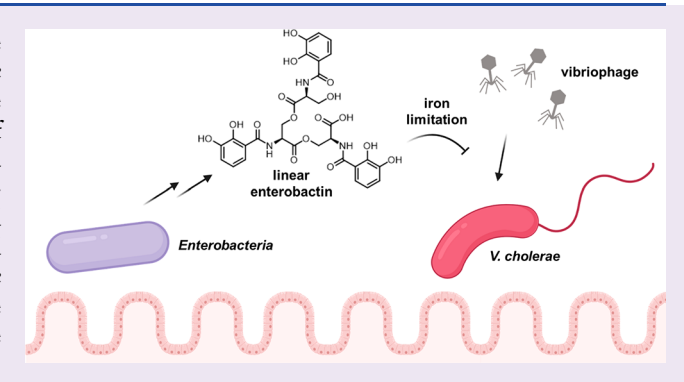
**ACCESS** I

III Metrics & More

Article Recommendations

Supporting Information

ABSTRACT: Vibrio cholerae is the causative agent of the severe diarrheal disease cholera. Bacteriophages that prey on *V. cholerae* may be employed as phage therapy against cholera. However, the influence of the chemical environment on the infectivity of vibriophages has been unexplored. Here, we discovered that a common metabolite produced by gut microbes—linear enterobactin (LinEnt), represses vibriophage proliferation. We found that the antiphage effect by LinEnt is due to iron sequestration and that multiple forms of iron sequestration can protect *V. cholerae* from phage predation. This discovery emphasizes the significance that the chemical environment can have on natural phage infectivity and phage-based interventions.



#### INTRODUCTION

Bacteriophages (phages) are viruses that infect bacteria. These naturally occurring viruses have been applied as "phage therapy" to treat bacterial infections since the early 20th century.¹ However, shortly after the discovery of penicillin,² administration of antibiotics overshadowed phage therapy as an antimicrobial strategy.³ Due to the recent global antibiotic resistance crisis,⁴ the world has seen a revived interest in phage therapy.⁵ Phages have many advantages over antibiotics for the treatment of bacterial infections, such as specificity of action and tunability by engineering.⁶ One obstacle to the employment of phage therapy is that some phages that efficiently kill bacteria under laboratory conditions are poor predators in the natural infection environment.<sup>7-9</sup>

One difference between laboratory conditions and natural conditions is the chemical environment. 10 In the laboratory, bacteria are often grown in monoculture in a defined nutrientrich media. In nature, phages must infect their prey bacteria within polymicrobial communities. These communities harbor a complex metabolic environment, including various secondary metabolites that can alter the physiology of the prey bacteria. 10,11 Additionally, these metabolites can alter phage infectivity. For example, anthracyclines and aminoglycosides produced by Streptomyces can directly interfere with phage reproduction in *Escherichia coli*,  $^{12-17}$  while  $\beta$ -lactams can stimulate virulent phage proliferation in E. coli. 18 Additionally, the metabolites mitomycin C, pyocyanin, and colibactin have been shown to trigger prophages in neighboring cells to enter their lytic cycles. 19-21 These findings suggest that environmental regulation of phage-host interactions by microbial metabolites could be common in nature. We hypothesized that

other microbial metabolites can influence phage infectivity with uncharacterized mechanisms.

For this study, we focused on phages that infect Vibrio cholerae—the causative agent of cholera<sup>22</sup> and a potential target for phage therapy. 23,24 Considering the complex metabolic environment in the gut where V. cholerae and vibriophages live,<sup>25</sup> we hypothesized that metabolites produced by other microbiome members or by the host itself can influence the infectivity of vibriophages. Prior to this work, the influence of microbial metabolites on the infectivity of vibriophages has been unexplored. Therefore, we screened a library of microbial chemical extracts to determine if any could influence the susceptibility of V. cholerae to its phages. We discovered that a common microbial siderophore, linear enterobactin (LinEnt), represses vibriophage proliferation. The antiphage effect of LinEnt was linked to iron starvation, which cautions that natural iron limitation may impact the success of many phage-based interventions.

# RESULTS

The Common Microbial Siderophore, Linear Enterobactin (LinEnt), Inhibits ICP1 Infection. An in-house library of microbial metabolite extracts was screened (Supporting Information) for the ability to promote or inhibit

Received: May 13, 2022 Accepted: August 10, 2022 Published: August 12, 2022





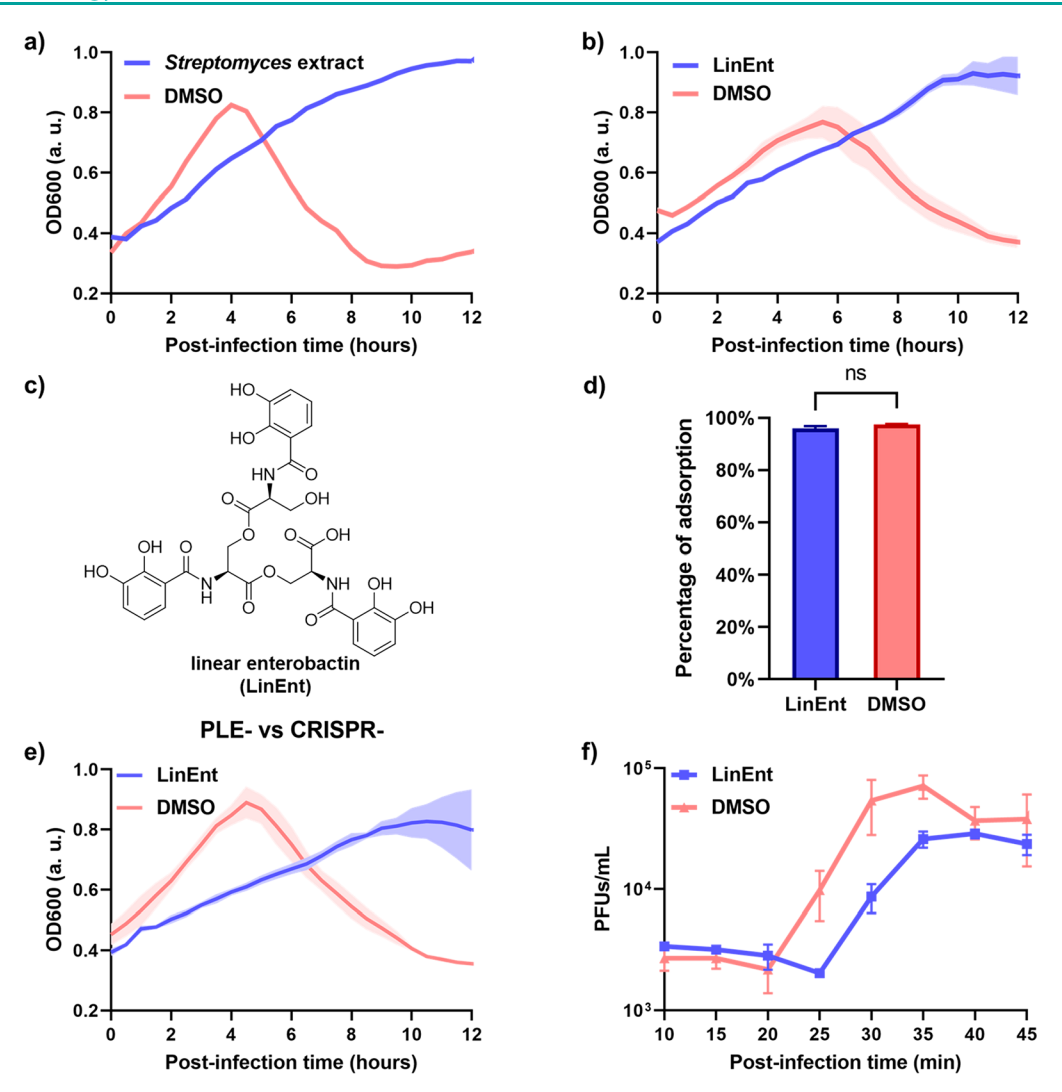


Figure 1. LinEnt represses ICP1 infection. (a) Growth curves of V. cholerae cultures infected with ICP1 phages (MOI =  $10^{-6}$ ) supplemented with 20  $\mu$ g of Streptomyces sp. metabolite extract or DMSO. (b) Growth curves of V. cholerae cultures infected with ICP1 phages (MOI =  $10^{-6}$ ) supplemented with 200  $\mu$ M LinEnt or DMSO. The growth curves represent the mean of three biological replicates, and the shaded area corresponds to the standard error of the mean. (c) The chemical structure of LinEnt. (d) The percentage of ICP1 phages adsorbed on V. cholerae cells treated with 200  $\mu$ M LinEnt or DMSO. Bars represent the mean of three biological replicates, and the error bars correspond to the standard error of the mean. (e) Growth curves of V. cholerae PLE $^-$  cultures infected with ICP1 CRISPR $^-$  phages (MOI =  $10^{-6}$ ) supplemented with 200  $\mu$ M LinEnt or DMSO. The growth curves represent the mean of two biological replicates, and the shaded area corresponds to the standard error of the mean. (f) The change of ICP1 concentration within one round of infection under the treatment of 200  $\mu$ M LinEnt or DMSO. Curves represent the mean of three biological replicates, and the error bars correspond to the standard error of the mean.

the lysis of *V. cholerae* by the common lytic *Myoviridae* phage ICP1. 26 *V. cholerae* was preincubated with the chemical extracts in microtiter plates prior to the addition of ICP1. Although no extracts were found to promote phage predation (data not shown), one extract was observed to protect *V. cholerae* from ICP1-induced lysis (Figure 1a). The producer of this compound was a previously isolated *Streptomyces* species (Supporting Information). Although the ecological relevance between *V. cholerae* and a soil-dwelling *Streptomyces* was unclear, we continued to identify the active metabolite.

Bioassay-guided fractionation was employed to isolate the active component(s) produced by the *Streptomyces* sp. We isolated a pure compound that was sufficient to protect V. cholerae from ICP1 (Figure 1b). High-resolution mass spectrometry of this compound revealed an m/z of 688.1619  $[M+H]^+$  (Figure S1). Tandem mass spectrometry (MS/MS) analysis of this compound (Figure S1) revealed a fragmenta-

tion pattern that matches substructures of linear enterobactin (LinEnt, Figure 1c), <sup>27</sup> a byproduct of enterobactin biosynthesis and utilization. <sup>28</sup> Subsequent 1D and 2D NMR spectroscopy analyses (Table S3, Figures S2–S6) confirmed that the active compound has an identical planar structure to that of linear enterobactin. <sup>29</sup> Optical rotation measurement ([ $\alpha$ ]<sub>D</sub><sup>23</sup> + 13, c 0.10, MeOH) confirmed that the absolute stereochemistry of LinEnt matched the published form, which is constructed from L-serine. <sup>29</sup>

Notably, LinEnt is also produced by *E. coli*,<sup>27</sup> a member of the gut microbiome. We isolated LinEnt from *E. coli* and confirmed that it was identical to the one isolated from the *Streptomyces* sp. (Figure S7). The LinEnt isolated from *E. coli* was then used to carry out further experiments.

**LinEnt Does Not Affect ICP1 Adsorption.** A common mechanism to inhibit phage infection is alteration of the cell surface, which inhibits phage adsorption. <sup>30–32</sup> For example,

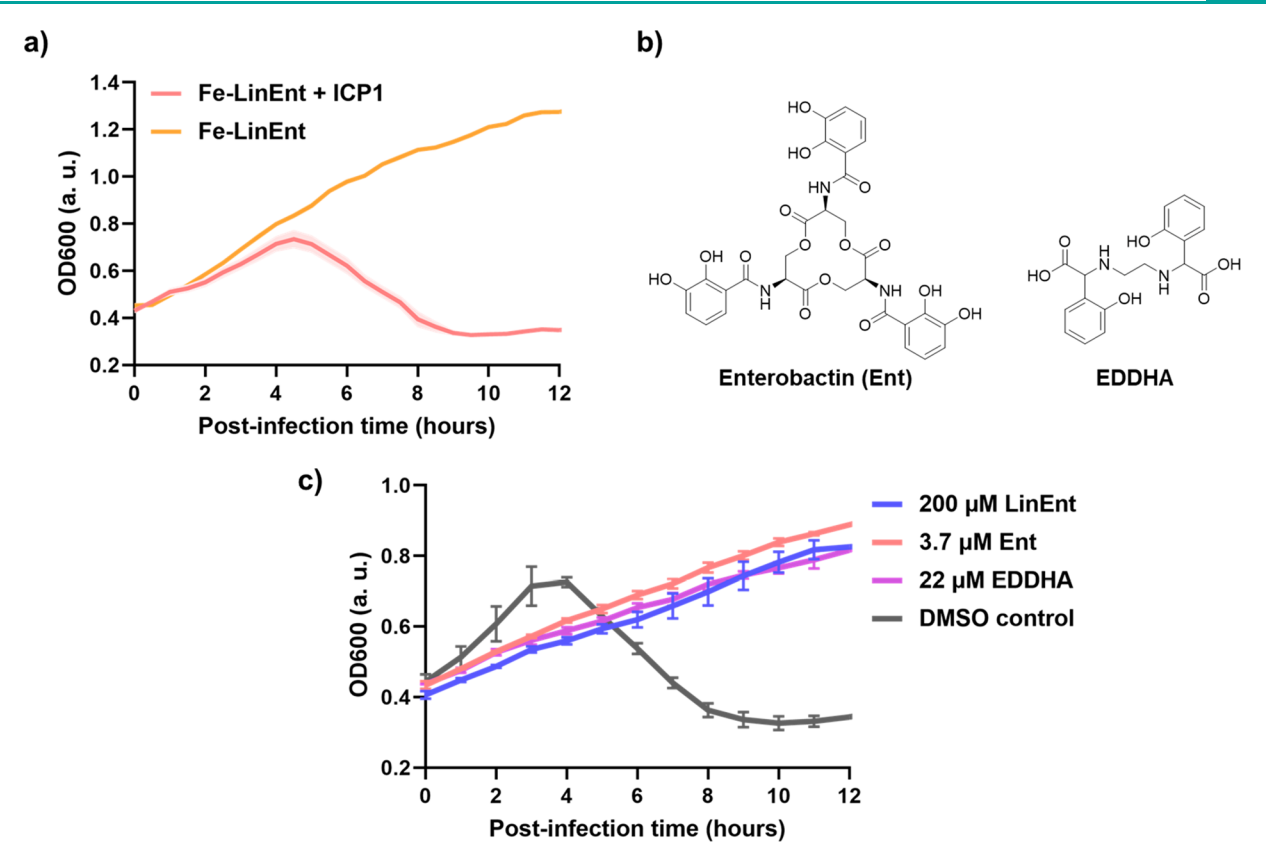


**Figure 2.** Iron sequestration generally inhibits ICP1 infection. (a) Growth curves of *V. cholerae* cultures in the presence of Fe-LinEnt when infected by ICP1 phages (MOI =  $10^{-6}$ ). The growth curves represent the mean of three biological replicates, and the shaded area corresponds to the standard error of the mean. (b) The chemical structures of Ent and EDDHA. (c) Growth curves of *V. cholerae* cultures infected with ICP1 phages (MOI =  $10^{-6}$ ) supplemented with 200  $\mu$ M LinEnt, 3.7  $\mu$ M Ent, 22  $\mu$ M EDDHA, or DMSO.

LinEnt might influence production of the O antigen, which serves as a receptor for ICP1. To determine if LinEnt inhibits ICP1 adsorption, we performed a phage adsorption assay. Briefly, ICP1 phages were allowed to adsorb onto *V. cholerae* cells, then the number of unadsorbed phages was enumerated, and the adsorption ratio was calculated. We observed no significant decrease in the phage adsorption ratio under LinEnt treatment compared to DMSO treatment (Figure 1d). In both cases, greater than 95% of the phages in the medium were able to adsorb to bacterial cells in 10 min, which agrees with reported data for ICP1. This result indicates that LinEnt does not inhibit ICP1 adsorption.

LinEnt Inhibition Does Not Function by Enhancing a Common V. cholerae Antiphage Defense. V. cholerae has a well-studied anti-ICP defense called Phage-induced chromosomal-Like Element (PLE) to which ICP phages have evolved CRISPR/Cas counter-defenses. To determine if LinEnt inhibits ICP1 by inducing PLE or inhibiting the phage CRISPR counter-defense, we tested if LinEnt inhibited ICP1 CRISPR—infection in a V. cholerae PLE—mutant. Indeed, LinEnt was still active (Figure 1e). Therefore, because LinEnt inhibits ICP1 regardless of the presence of PLE and CRISPR, LinEnt does not function by altering the balance of the competition between the PLE defense and the CRISPR counterdefense.

**LinEnt Delays Cell Lysis and Reduces Phage Burst Size.** Since linear enterobactin does not inhibit ICP1 adsorption to *V. cholerae*, the antiphage effect is likely due to disrupting phage proliferation after the adsorption step. The "latent period" and "burst size" are key parameters character-

izing the phage infection process. The latent period is the time required for phages to lyse the host cell and produce new progeny. Burst size measures the productivity of a phage, which is defined as the number of new phages released from each infected bacterial cell. Therefore, we measured the latent period and burst size by monitoring the change of phage concentration after one round of infection (Figure 1f), 36 in the presence and absence of LinEnt treatment. After LinEnt treatment, the latent period increased from 20 to 25 min (Figure 1f), indicating that ICP1-mediated cell lysis was delayed by 5 min. Meanwhile, under LinEnt treatment, phage burst size decreased from  $20 \pm 3$  to  $9.7 \pm 0.5$  (Figure 1f), meaning that fewer phages were released from each infected bacterial cell. Based on mathematical modeling, this modest delay of cell lysis and decrease of burst size can account for a substantial inhibitory effect after multiple generations of phage replication (Supplemental Text and Table S4). Ultimately, LinEnt enabled the bacterial population to reach the stationary phase before the phage destroyed the population (Figure 1b). Since the phage infections were only weakened but not completely arrested, infection with a large number of phages should overcome the effect of LinEnt. Indeed, phages began to overcome the effect of LinEnt at a multiplicity of infection (MOI)  $\sim$  0.001, while addition of ICP1 at a MOI  $\sim$  1 completely lysed the culture (Figure S8).

Inhibition by LinEnt Is Due to Iron Sequestration. Because LinEnt is a siderophore produced by certain *Streptomyces* spp. and *E. coli*,<sup>27,29</sup> we hypothesized that it inhibits phage proliferation by sequestering iron away from *V. cholerae*. To test if the phage inhibition was the result of iron

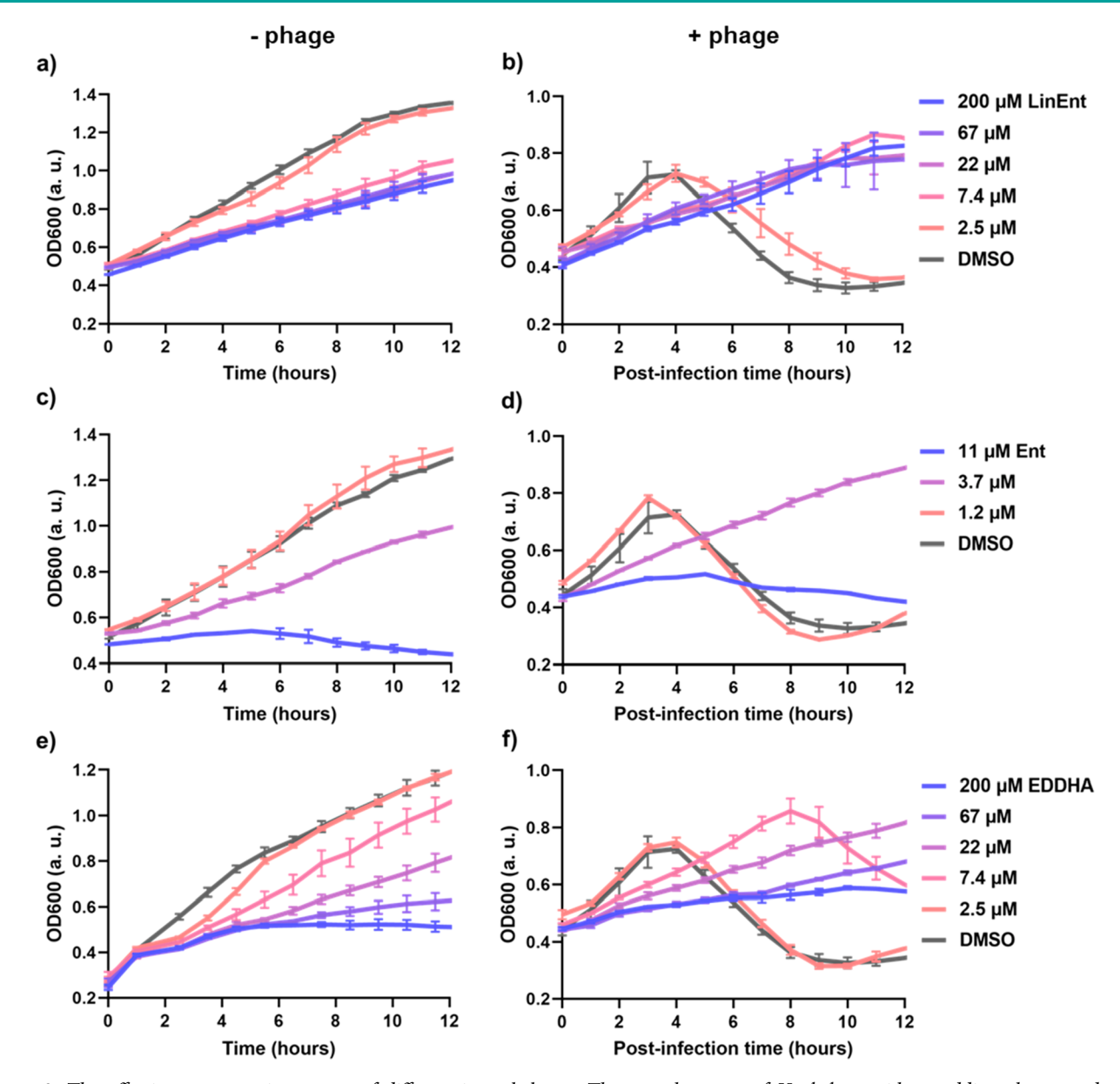


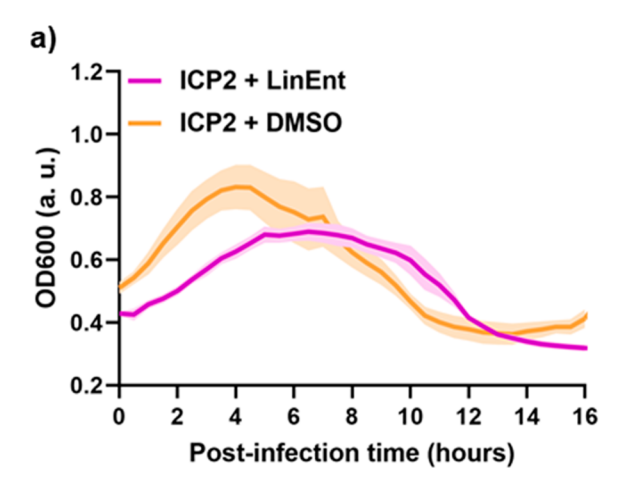
**Figure 3.** The effective concentration ranges of different iron chelators. The growth curves of V. cholerae without adding phages under the treatment of (a) LinEnt, (c) Ent, or (e) EDDHA. The growth curves of V. cholerae infected by ICP1 phages (MOI =  $10^{-6}$ ) in the presence of (b) LinEnt, (d) Ent, or (f) EDDHA. Curves represent the mean of three biological replicates, and the error bars correspond to the standard error of the mean.

sequestration by LinEnt, we saturated LinEnt with iron and added this Fe-LinEnt complex to *V. cholerae* culture prior to phage infection. As expected, the Fe-LinEnt complex—which is incapable of sequestering iron—was unable to inhibit ICP1 infection (Figure 2a). Therefore, we concluded that the antiphage activity of LinEnt was due to iron sequestration.

Other Iron Scavengers Inhibit ICP1 Proliferation. Since LinEnt represses ICP1 infection by sequestering iron away from V. cholerae, we hypothesized that other iron chelators have a similar effect. We thus investigated two other iron chelators—enterobactin (Ent) and ethylenediamine-N,N'-bis (2-hydroxyphenyl-acetic acid) (EDDHA; Figure 2b). Ent is the nonhydrolyzed macrocyclic analog of LinEnt, while EDDHA is a synthetic compound commonly used to sequester iron in laboratory studies.<sup>37</sup> As expected, ICP1 propagation was repressed by Ent (3.7  $\mu$ M) and EDDHA (22

 $\mu$ M; Figure 2c). Therefore, multiple methods of iron sequestration can protect V. cholerae from ICP1.

LinEnt Exhibits a Uniquely Wide Range of Protective Concentrations. We noticed that LinEnt, Ent, and EDDHA all slowed the growth rate of V. cholerae at their antiphage concentrations (Figure 2c). The decreased growth rate can be observed in the absence of phages, as well (Figure 3a,c,e). For LinEnt, the minimal concentration for phage inhibition correlates with the minimal concentration for slowing growth ( $\sim 7~\mu M$ ; Figure 3a,b). We also tested a range of concentrations of Ent and EDDHA (Figure 3c–f). In contrast to a more than 30-fold effective range of LinEnt spanning from  $7~\mu M$  to 200  $\mu M$  (Figure 3b), Ent and EDDHA exhibited a very tight window of antiphage activity (Figure 3d,f). Ent and EDDHA arrested bacterial growth at higher concentrations, presumably because they limit iron availability too strongly (Figure 3c,e). LinEnt slowed bacterial growth but did not



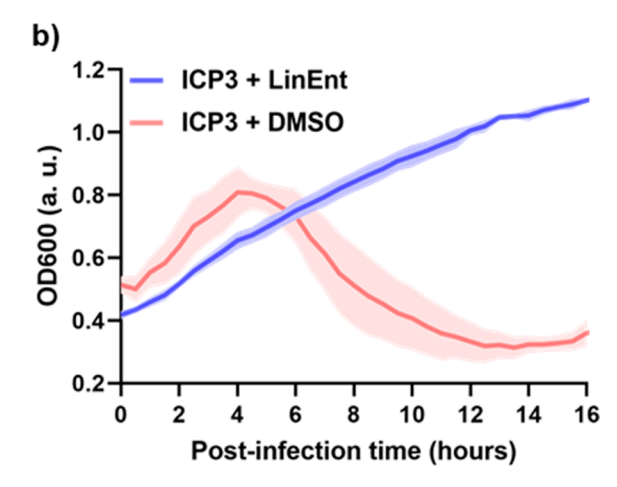


Figure 4. LinEnt also protects V. cholerae from the ICP3 phage. Growth curves of V. cholerae cultures infected with (a) ICP2 phages (MOI =  $10^{-5}$ ) and (b) ICP3 phages (MOI =  $10^{-5}$ ) after treatment with 200  $\mu$ M of LinEnt or DMSO. The growth curves represent the mean of three biological replicates, and the shaded area corresponds to the standard error of the mean.

completely halt it. This trait is likely because *V. cholerae* can salvage iron bound to LinEnt—the *V. cholerae* receptors ViuA, VctA, and IrgA have been shown to import ferric-LinEnt but not ferric-Ent under iron-limited conditions.<sup>38</sup> Our growth inhibition data suggest that ferric-LinEnt is not the most efficient means of iron import for *V. cholerae*, but it still allows moderate *V. cholerae* growth. Therefore, LinEnt is a privileged chelator that provides phage protection over a wide concentration range; however, the enterobactin and EDDHA results suggest that any form of iron limitation can protect *V. cholerae* from ICP1.

LinEnt Also Protects *V. cholerae* from Other ICP Phages. In addition to ICP1, two less prevalent lytic vibriophages, ICP2 (*Podoviridae*) and ICP3 (*Podoviridae*), have been isolated from clinical *V. cholerae* samples.<sup>25</sup> To explore the generality of the antiphage effect of LinEnt, we tested if either of these two phages is also inhibited by LinEnt. LinEnt protected *V. cholerae* well from ICP3; however, ICP2 was significantly less sensitive to LinEnt (Figure 4). To determine if ICP2 was generally less sensitive to iron limitation, we also tested EDDHA (Figure S9). Indeed, ICP2 was only weakly inhibited by EDDHA. Therefore, LinEnt (and iron limitation in general) can protect *V. cholerae* to different extents from multiple phages.

## DISCUSSION

We have discovered that linear enterobactin, a common siderophore produced by  $E.\ coli^{27}$  and some Streptomyces species can repress vibriophage proliferation through iron sequestration. We suggest that this mechanism of interspecies iron competition may pose a challenge for the application of vibriophages as interventions against cholera and may represent a general limitation of phage-based therapy in clinical use.

Vibriophages have proven effective in decreasing the severity of cholera in animal infection models. <sup>23,24</sup> However, phage-susceptible *V. cholerae* could still be isolated from guts after phage treatment, suggesting a transient phage resistance mechanism. <sup>23</sup> Yen et al. attributed the persistence of *V. cholerae* to the spatial complexity of the gut, which can limit encounters between phages and bacteria. <sup>23</sup> Our data suggest another possibility: the chemical environment in guts may confer *V. cholerae* transient resistance to its phages. *E. coli* and

other enterobactin producing bacteria are commonly present in the gut microbiome, albeit at low concentrations. <sup>39</sup> In fact, their levels can increase following V. *cholerae* infection. <sup>40,41</sup> In pure culture, strains of E. *coli* have produced greater than 200  $\mu$ M enterobactin (which readily hydrolyzes into LinEnt). <sup>42</sup> Furthermore, enterobactin has been observed in animal guts. <sup>43</sup> Therefore, it is plausible that the hydrolyzed product of enterobactin, LinEnt, exists in guts at concentrations sufficient (>10  $\mu$ M) to repress vibriophage infection.

Furthermore, we found that other iron chelators reproduce the antiphage effect—albeit with a narrower concentration range before they completely inhibit V. cholerae growth. Although it is difficult to measure the amount of available iron in the gut, it is likely that substantial competition for iron exists. Many gut microbes express siderophores, 44 and the host gut mucosa is rich in iron-sequestering proteins such as lipocalin-2 (Lcn2) during inflammation. 45,46 Therefore, beyond the specific effect of LinEnt, other mechanisms of iron sequestration may inhibit vibriophage infectivity in the gut. Nonetheless, it is notable that LinEnt inhibits phage proliferation at a wider concentration range without completely arresting V. cholerae growth compared to enterobactin and EDDHA. LinEnt is unique because V. cholerae can import and salvage some iron from ferric-LinEnt.<sup>38,47</sup> Further studies are warranted to evaluate the significance of LinEnt or other forms of iron sequestration for vibriophage interventions in animal models. Our results predict that the effect will be greatest when low concentrations of phages are employed.

Two of the three examined vibriophages (ICP1 and ICP3) were strongly inhibited by LinEnt, while the effect on ICP2 was weaker. The mechanism by which ICP2 evades inhibition is an intriguing topic for further study. Its replication may be less sensitive to iron concentration. Alternatively, iron limitation may have a counteracting phage-promoting effect for ICP2—for example by increasing expression of its receptor in *V. cholerae*. Regardless, the result demonstrates that iron limitation can generally inhibit vibriophage proliferation.

The exact mechanism by which iron limitation inhibits vibriophage proliferation remains unclear. Our experiments rule out effects on adsoption or on the *V. cholerae* PLE defense and phage CRISPR counterdefense. Although iron limitation both slows *V. cholerae* growth and inhibits vibriophage replication, one might hypothesize that other forms of growth

inhibition generally inhibit phage replication and protect the host. However, several antibiotics failed to inhibit phage replication at concentrations where they slowed bacterial growth (Figure S10). Only some aminoglycosides protected V. cholerae from phages (Figure S11)—a result previously noted in E. coli and suspected to involve unique interactions with the phage DNA. 15-17 Therefore, we hypothesize that the modest iron limitation caused by LinEnt inhibits a process that is more important for phage replication than for bacterial replication. One hypothetical target is the iron-dependent ribonucleotide reductase (RNR) enzymes, which generate deoxyribonucleotides. Phages need an abundance of deoxyribonucleotides to rapidly replicate their genomes—evidenced by the frequent occurrence of RNR genes on phage genomes. 48 The best annotated ICP phage genome (ICP1) encodes both a type I and a type III RNR.<sup>48</sup> Therefore, a slight decrease in available intracellular iron could lead to fewer active RNR enzymes, 49,50 a depleted pool of deoxyribonucleotides, and therefore lower replication of phage genomes. Further studies are necessary to test this hypothesis and consider the involvement of other iron-dependent processes.

Beyond vibriophages, we posit that this antiphage protection of bacteria by iron sequestration is a mechanism of physiological refuge that may broadly inhibit phage-based interventions on many bacterial species. The term "physiological refuge" explains how bacteria that remain genetically susceptible to a phage can survive: a portion of the (or the entire) bacterial population sometimes enters a physiological state that is recalcitrant to phage infection.<sup>51</sup> Physiological refuge is mostly discussed in terms of a modified cell wall or calcium starvation. 52,53 However, iron starvation is a common occurrence that impacts the rates of the tricarboxylic acid cycle and DNA biosynthesis in bacteria.<sup>54</sup> Therefore, the efficiency with which many phages infect their hosts may be greatly diminished in natural iron-limited environments. Indeed, another study showed that supplementing iron in a metal deficient condition can stimulate phage infection of E. coli.8 This hypothesis is not universal, though, as some phages may infect bacteria better under iron starvation, notably in cases where the phages dock onto the bacterial siderophore receptors, which are frequently upregulated during iron starvation.<sup>54</sup> Therefore, the availability of iron ions in each environment may determine the susceptibility of many bacteria to their multitude of phages.

In conclusion, we have found a new natural productbacteriophage interaction that weakens the efficacy of lytic phages that kill V. cholerae, the causative agent of cholera. Importantly, this natural product is prevalent in both environmental and host-associated microbiomes, where V. cholerae exists. This observation emphasizes the significance that the chemical environment can have on natural phage infectivity and phage-based interventions.

# METHODS

Safety Statement. Caution! V. cholerae was handled following BSL 2 protocols.

Strains and Growth Conditions. The strains and bacteriophages used in this study are listed in Table S1. All of the chemicals used in this study are listed in Table S2. V. cholerae strains were routinely grown in LB broth supplemented with 100  $\mu$ g/mL of streptomycin at 37 °C and 220 rpm. To obtain a log-phase V. cholerae culture, an overnight culture was diluted 1:50 into fresh LB broth and incubated at 37 °C and 220 rpm for 1.5 h until the optical density at 600 nm

(OD<sub>600</sub>) reached 0.3-0.4 (1 cm path length). A detailed description of phage preparation can be found in the Supporting Information.

Antiphage Activity Test. The tested compound was dissolved in DMSO, and 2  $\mu$ L was added into a microtiter well of a 96-well plate. A total of 180  $\mu$ L of log-phase *V. cholerae* KS393 (OD<sub>600</sub> 0.3–0.4) was added into the well and incubated at 37 °C for 2 h. Then, ~100 plaque forming units (PFUs) of phages were added into the compound-treated bacteria (MOI =  $10^{-6}$ ). The plate was incubated at 37 °C in a Biospa8 (Biotek), and the OD<sub>600</sub> was recorded every 30 min for 20 h using a Synergy H1 plate reader (Biotek).

Growth Inhibition Test of V. cholerae. The tested compound was dissolved in DMSO, and 2  $\mu$ L was added into a microtiter well of a 96-well plate. Then, 200  $\mu L$  of log-phase V. cholerae KS393 (OD<sub>600</sub> 0.3-0.4) was added into the well. The plate was incubated at 37 °C in a Biospa8, and the OD<sub>600</sub> was recorded every 30 min for 20 h using a Synergy H1 plate reader.

Adsorption Assay. A total of 180 µL of log-phase V. cholerae KS393 ( $10^8$  colony forming units[CFUs]/mL) was mixed with 2  $\mu$ L of 20 mM linear enterobactin DMSO solution or 2  $\mu L$  of DMSO and incubated at 37 °C for 2 h. Then, 20 µL of ICP1 phage (10<sup>5</sup> PFUs) was added to the treated bacteria and incubated for 10 min to allow adsorption. The culture was then centrifuged at 4 °C and 16 000g for 2 min to pellet the bacteria with adsorbed phages. The supernatant was collected and treated with 20  $\mu$ L of chloroform. The number of unadsorbed phages in the aqueous layer was measured by the soft agar overlay method (Supporting Information). The adsorption ratio was calculated by the following equation:

Adsorption ratio

$$= \frac{\text{(# of phages added - # of unadsorbed phages)}}{\text{# of phages added}} \times 1009$$

One-Step Growth Curve Measurement. This protocol was adapted from the one reported by Kropinski. 36 Briefly, 900 µL of logphase V. cholerae KS393 (OD<sub>600</sub> 0.3-0.4) was added to a culture tube and then incubated with 10  $\mu$ L of DMSO or 10  $\mu$ L of 20 mM LinEnt DMSO solution at 37 °C for 2 h. After the treatment, 100  $\mu$ L of ICP1 phage ( $\sim$ 1000 PFUs, MOI =  $10^{-5}$ ) was added to the tube and kept at 37 °C. After 10 min of adsorption, 150  $\mu$ L of the culture was removed and treated with 20  $\mu$ L of chloroform. This sample was placed in ice and titrated in the end to determine the number of infected cells. At 10 min postinfection, 100  $\mu$ L of the culture was mixed with 100  $\mu$ L of V. cholerae KS393. The mixture was serially diluted, added into 3 mL of melted LB + 0.5% agar, and poured onto a prewarmed LB + 1.5%agar plate. The culture was sampled every 5 min afterward, and the step above was repeated. The plates were incubated at 37 °C for 6 h, and the number of plaques was enumerated. The phage concentration in the culture was calculated based on the number of plaques counted.

High-Throughput Screening and Isolation of LinEnt. A detailed description of high-throughput screening for the anti-ICP1 metabolite, isolation, and characterization of LinEnt can be found in the Supporting Information.

## ASSOCIATED CONTENT

# Supporting Information

The Supporting Information is available free of charge at https://pubs.acs.org/doi/10.1021/acschembio.2c00422.

Additional information regarding experimental methods, MS/MS spectrum, NMR spectra, and supplementary results (PDF)

# AUTHOR INFORMATION

## **Corresponding Author**

Joseph P. Gerdt - Department of Chemistry, Indiana University, Bloomington, Indiana 47405, United States; orcid.org/0000-0002-0375-4110; Email: jpgerdt@ iu.edu

#### **Authors**

Zhiyu Zang — Department of Chemistry, Indiana University, Bloomington, Indiana 47405, United States; orcid.org/0000-0002-4879-7077

**Kyoung Jin Park** – Department of Chemistry, Indiana University, Bloomington, Indiana 47405, United States

Complete contact information is available at: https://pubs.acs.org/10.1021/acschembio.2c00422

#### **Notes**

The authors declare no competing financial interest.

## ACKNOWLEDGMENTS

We thank K. Seed (University of California-Berkeley) for advice and for providing V. cholerae bacteria and phages. We thank A. Camilli (Tufts University) for providing V. cholerae bacteria and phages. We thank J. Henderson (Washington University in St. Louis) for providing E. coli UTI89. We thank E. M. Nolan (Massachusetts Institute of Technology) for providing enterobactin. We thank D. Schwartz (Indiana University) for comments on previous versions of the manuscript. The research was supported by a research starter grant from the American Society of Pharmacognosy to J.P.G. and an NSF CAREER award (IOS-2143636 to J.P.G.). Z.Z. was supported in part by the John R. and Wendy L. Kindig Fellowship. K.J.P. and the Laboratory for Biological Mass Spectrometry were supported by the Indiana University Precision Health Initiative. The 500 MHz NMR and 600 MHz spectrometer of the Indiana University NMR facility were supported by NSF grant CHE-1920026, and the Prodigy probe was purchased in part with support from the Indiana Clinical and Translational Sciences Institute funded, in part, by NIH Award TL1TR002531.

#### REFERENCES

- (1) d'Herelle, F. Bacteriophage as a treatment in acute medical and surgical infections. *Bull. N.Y. Acad. Med.* **1931**, 7 (5), 329–348.
- (2) Fleming, A. On the antibacterial action of cultures of a penicillium, with special reference to their use in the isolation of *B. influenzæ. Br. J. Exp. Pathol.* **1929**, *10* (3), 226–236.
- (3) Summers, W. C. Bacteriophage therapy. *Annu. Rev. Microbiol.* **2001**, 55 (1), 437–451.
- (4) Blair, J. M. A.; Webber, M. A.; Baylay, A. J.; Ogbolu, D. O.; Piddock, L. J. V. Molecular mechanisms of antibiotic resistance. *Nature Reviews Microbiology* **2015**, *13* (1), 42–51.
- (5) Dedrick, R. M.; Guerrero-Bustamante, C. A.; Garlena, R. A.; Russell, D. A.; Ford, K.; Harris, K.; Gilmour, K. C.; Soothill, J.; Jacobs-Sera, D.; Schooley, R. T.; et al. Engineered bacteriophages for treatment of a patient with a disseminated drug-resistant *Mycobacterium abscessus*. *Nature Medicine* **2019**, 25 (5), 730–733.
- (6) Principi, N.; Silvestri, E.; Esposito, S. Advantages and limitations of bacteriophages for the treatment of bacterial infections. *Front. Pharmacol.* **2019**, *10*, 513.
- (7) Weiss, M.; Denou, E.; Bruttin, A.; Serra-Moreno, R.; Dillmann, M.-L.; Brüssow, H. In vivo replication of T4 and T7 bacteriophages in germ-free mice colonized with *Escherichia coli*. *Virology* **2009**, 393 (1), 16–23.
- (8) Ma, L.; Green, S. I.; Trautner, B. W.; Ramig, R. F.; Maresso, A. W. Metals enhance the killing of bacteria by bacteriophage in human blood. *Sci. Rep.* **2018**, *8* (1), 2326.
- (9) Suh, G. A.; Lodise, T. P.; Tamma, P. D.; Knisely, J. M.; Alexander, J.; Aslam, S.; Barton, K. D.; Bizzell, E.; Totten, K. M. C.; Campbell, J. L.; Chan, B. K.; Cunningham, S. A.; Goodman, K. E.; Greenwood-Quaintance, K. E.; Harris, A. D.; Hesse, S.; Maresso, A.; Nussenblatt, V.; Pride, D.; Rybak, M. J.; Sund, Z.; van Duin, D.; Van

- Tyne, D.; Patel, R. Considerations for the use of phage therapy in clinical practice. *Antimicrob. Agents Chemother.* **2022**, *66* (3), e0207121.
- (10) Davies, J.; Ryan, K. S. Introducing the parvome: Bioactive compounds in the microbial world. *ACS Chem. Biol.* **2012**, 7 (2), 252–259.
- (11) Hibbing, M. E.; Fuqua, C.; Parsek, M. R.; Peterson, S. B. Bacterial competition: Surviving and thriving in the microbial jungle. *Nature Reviews Microbiology* **2010**, 8 (1), 15–25.
- (12) Schatz, A.; Jones, D. The production of antiphage agents by actinomycetes. *Bulletin of the Torrey Botanical Club* **1947**, 74 (1), 9–19.
- (13) Osada, H. Fascinating bioactive compounds from actinomycetes. *Actinomycetologica* **1995**, *9* (2), 254–262.
- (14) Kronheim, S.; Daniel-Ivad, M.; Duan, Z.; Hwang, S.; Wong, A. I.; Mantel, I.; Nodwell, J. R.; Maxwell, K. L. A chemical defence against phage infection. *Nature* **2018**, *564* (7735), 283–286.
- (15) Jiang, Z.; Wei, J.; Liang, Y.; Peng, N.; Li, Y. Aminoglycoside antibiotics inhibit mycobacteriophage infection. *Antibiotics* **2020**, 9 (10), 714.
- (16) Zuo, P.; Yu, P.; Alvarez, P. J. J. Aminoglycosides antagonize bacteriophage proliferation, attenuating phage suppression of bacterial growth, biofilm formation, and antibiotic resistance. *Appl. Environ. Microbiol.* **2021**, *87* (15), e00468-21.
- (17) Kever, L.; Hardy, A.; Luthe, T.; Hunnefeld, M.; Gatgens, C.; Milke, L.; Wiechert, J.; Wittmann, J.; Moraru, C.; Marienhagen, J.; Frunzke, J. Aminoglycoside antibiotics inhibit phage infection by blocking an early step of the infection cycle. *mBio* **2022**, *13* (3), e00783–22.
- (18) Comeau, A. M.; Tétart, F.; Trojet, S. N.; Prère, M.-F.; Krisch, H. M. Phage-antibiotic synergy (PAS):  $\beta$ -Lactam and quinolone antibiotics stimulate virulent phage growth. *PLoS One* **2007**, 2 (8), e799.
- (19) Jancheva, M.; Böttcher, T. A metabolite of *Pseudomonas* triggers prophage-selective lysogenic to lytic conversion in *Staphylococcus aureus*. *J. Am. Chem. Soc.* **2021**, *143* (22), 8344–8351.
- (20) Otsuji, N.; Sekiguchi, M.; Iijima, T.; Takagi, Y. Induction of phage formation in the lysogenic *Escherichia coli* K-12 by mitomycin C. *Nature* **1959**, *184* (4692), 1079–1080.
- (21) Silpe, J. E.; Wong, J. W. H.; Owen, S. V.; Baym, M.; Balskus, E. P. The bacterial toxin colibactin triggers prophage induction. *Nature* **2022**, *603*, 315.
- (22) Clemens, J. D.; Nair, G. B.; Ahmed, T.; Qadri, F.; Holmgren, J. Cholera. *Lancet* **2017**, *390* (10101), 1539–1549.
- (23) Yen, M.; Cairns, L. S.; Camilli, A. A cocktail of three virulent bacteriophages prevents *Vibrio cholerae* infection in animal models. *Nat. Commun.* **2017**, 8 (1), 14187.
- (24) Bhandare, S.; Colom, J.; Baig, A.; Ritchie, J. M.; Bukhari, H.; Shah, M. A.; Sarkar, B. L.; Su, J.; Wren, B.; Barrow, P.; et al. Reviving phage therapy for the treatment of cholera. *Journal of Infectious Diseases* **2019**, 219 (5), 786–794.
- (25) Seed, K. D.; Bodi, K. L.; Kropinski, A. M.; Ackermann, H.-W.; Calderwood, S. B.; Qadri, F.; Camilli, A. Evidence of a dominant lineage of *Vibrio cholerae*-specific lytic bacteriophages shed by cholera patients over a 10-year period in Dhaka, Bangladesh. *mBio* **2011**, 2 (1), e00334-10.
- (26) Boyd, C. M.; Angermeyer, A.; Hays, S. G.; Barth, Z. K.; Patel, K. M.; Seed, K. D. Bacteriophage ICP1: A persistent predator of *Vibrio cholerae*. *Annual Review of Virology* **2021**, 8 (1), 285–304.
- (27) O'Brien, I. G.; Gibson, F. The structure of enterochelin and related 2,3-dihydroxy-N-benzoyne conjugates from *Eschericha coli*. *Biochimica et Biophysica Acta* (BBA) General Subjects **1970**, 215 (2), 393–402.
- (28) Raymond, K. N.; Dertz, E. A.; Kim, S. S. Enterobactin: An archetype for microbial iron transport. *Proc. Natl. Acad. Sci. U. S. A.* **2003**, *100* (7), 3584–3588.
- (29) Igarashi, Y.; Iida, T.; Fukuda, T.; Miyanaga, S.; Sakurai, H.; Saiki, I.; Miyanouchi, K. Catechoserine, a new catecholate-type

inhibitor of tumor cell invasion from Streptomyces sp. Journal of Antibiotics 2012, 65 (4), 207–209.

- (30) Hampton, H. G.; Watson, B. N. J.; Fineran, P. C. The arms race between bacteria and their phage foes. *Nature* **2020**, *577* (7790), 327–336
- (31) Destoumieux-Garzón, D.; Duquesne, S.; Peduzzi, J.; Goulard, C.; Desmadril, M.; Letellier, L.; Rebuffat, S.; Boulanger, P. The iron–siderophore transporter FhuA is the receptor for the antimicrobial peptide microcin J25: Role of the microcin Vall1–Pro16  $\beta$ -hairpin region in the recognition mechanism. *Biochem. J.* **2005**, 389 (3), 869–876.
- (32) Rabsch, W.; Ma, L.; Wiley, G.; Najar, F. Z.; Kaserer, W.; Schuerch, D. W.; Klebba, J. E.; Roe, B. A.; Gomez, J. A. L.; Schallmey, M.; et al. FepA- and TonB-dependent bacteriophage H8: Receptor binding and genomic sequence. *J. Bacteriol.* **2007**, *189* (15), 5658–5674.
- (33) Seed, K. D.; Faruque, S. M.; Mekalanos, J. J.; Calderwood, S. B.; Qadri, F.; Camilli, A. Phase variable O antigen biosynthetic genes control expression of the major protective antigen and bacteriophage receptor in *Vibrio cholerae* O1. *PLOS Pathogens* **2012**, 8 (9), e1002917.
- (34) Silva-Valenzuela, C. A.; Camilli, A. Niche adaptation limits bacteriophage predation of *Vibrio cholerae* in a nutrient-poor aquatic environment. *Proc. Natl. Acad. Sci. U. S. A.* **2019**, *116* (5), 1627–1632.
- (35) O'Hara, B. J.; Barth, Z. K.; McKitterick, A. C.; Seed, K. D. A highly specific phage defense system is a conserved feature of the *Vibrio cholerae* mobilome. *PLOS Genetics* **2017**, *13* (6), e1006838.
- (36) Kropinski, A. M. Practical advice on the one-step growth curve. In *Bacteriophages: Methods and Protocols*; Clokie, M. R. J., Kropinski, A. M., Lavigne, R., Eds.; Springer: New York, 2018; Vol. 3, pp 41–47.
- (37) Rogers, H. J. Iron-binding catechols and virulence in *Escherichia coli*. *Infect. Immun.* **1973**, 7 (3), 445–456.
- (38) Wyckoff, E. E.; Allred, B. E.; Raymond, K. N.; Payne, S. M. Catechol siderophore transport by *Vibrio cholerae*. *J. Bacteriol.* **2015**, 197 (17), 2840–2849.
- (39) Eckburg, P. B.; Bik, E. M.; Bernstein, C. N.; Purdom, E.; Dethlefsen, L.; Sargent, M.; Gill, S. R.; Nelson, K. E.; Relman, D. A. Diversity of the human intestinal microbial flora. *Science* **2005**, 308 (5728), 1635–1638.
- (40) Gorbach, S. L.; Banwell, J. G.; Jacobs, B.; Chatterjee, B. D.; Mitra, R.; Brigham, K. L.; Neogy, K. N. Intestinal microftora in asiatic cholera. I. "rice-water" stool. *Journal of Infectious Diseases* **1970**, *121* (1), 32–37.
- (41) Hsiao, A.; Ahmed, A. M. S.; Subramanian, S.; Griffin, N. W.; Drewry, L. L.; Petri, W. A.; Haque, R.; Ahmed, T.; Gordon, J. I. Members of the human gut microbiota involved in recovery from *Vibrio cholerae* infection. *Nature* **2014**, *515* (7527), 423–426.
- (42) Seiffert, A.; Goeke, K.; Fielder, H.-P.; Zähner, H. Production of the siderophore enterobactin: Use of four different fermentation systems and identification of the compound by HPLC. *Biotechnol. Bioeng.* 1993, 41 (2), 237–244.
- (43) Pi, H.; Jones, S. A.; Mercer, L. E.; Meador, J. P.; Caughron, J. E.; Jordan, L.; Newton, S. M.; Conway, T.; Klebba, P. E. Role of catecholate siderophores in gram-negative bacterial colonization of the mouse gut. *PLoS One* **2012**, *7* (11), e50020.
- (44) Hider, R. C.; Kong, X. Chemistry and biology of siderophores. *Natural Product Reports* **2010**, 27 (5), 637–657.
- (45) Wilson, B. R.; Bogdan, A. R.; Miyazawa, M.; Hashimoto, K.; Tsuji, Y. Siderophores in iron metabolism: From mechanism to therapy potential. *Trends in Molecular Medicine* **2016**, 22 (12), 1077–1090.
- (46) Moschen, A. R.; Adolph, T. E.; Gerner, R. R.; Wieser, V.; Tilg, H. Lipocalin-2: A master mediator of intestinal and metabolic inflammation. *Trends in Endocrinology & Metabolism* **2017**, 28 (5), 388–397.
- (47) Byun, H.; Jung, I.-J.; Chen, J.; Larios Valencia, J.; Zhu, J. Siderophore piracy enhances *Vibrio cholerae* environmental survival and pathogenesis. *Microbiology* **2020**, *166* (11), 1038–1046.

- (48) Dwivedi, B.; Xue, B.; Lundin, D.; Edwards, R. A.; Breitbart, M. A bioinformatic analysis of ribonucleotide reductase genes in phage genomes and metagenomes. *BMC Evolutionary Biology* **2013**, *13* (1), 33.
- (49) Torrents, E.; Buist, G.; Liu, A.; Eliasson, R.; Kok, J.; Gibert, I.; Gräslund, A.; Reichard, P. The anaerobic (class III) ribonucleotide reductase from *Lactococcus lactis*: Catalytic properties and allosteric regulation of the pure enzyme system. *J. Biol. Chem.* **2000**, 275 (4), 2463–2471.
- (50) Martin, J. E.; Imlay, J. A. The alternative aerobic ribonucleotide reductase of *Escherichia coli*, NrdEF, is a manganese-dependent enzyme that enables cell replication during periods of iron starvation. *Mol. Microbiol.* **2011**, *80* (2), 319–334.
- (51) Lenski, R. E., Dynamics of interactions between bacteria and virulent bacteriophage. In *Advances in Microbial Ecology*, Marshall, K. C., Ed.; Springer US: Boston, MA, 1988; pp 1–44.
- (52) Paynter, M. J. B.; Bungay, H. R., III Capsular protection against virulent coliphage infection. *Biotechnol. Bioeng.* **1970**, *12* (3), 341–346.
- (53) Luria, S. E.; Steiner, D. L. The role of calcium in the penetration of bacteriophage T5 into its host. *J. Bacteriol.* **1954**, *67* (6), 635–639.
- (54) Andrews, S. C.; Robinson, A. K.; Rodríguez-Quiñones, F. Bacterial iron homeostasis. *FEMS Microbiology Reviews* **2003**, 27 (2–3), 215–237.